Positron lifetime spectroscopy and decomposition processes in commercial Al-Zn-Mg-based alloys

1998 J. Phys.: Condens. Matter 10 3903

(http://iopscience.iop.org/0953-8984/10/17/019)

J. Phys.: Condens. Matter **10** (1998) 3903–3918. Printed in the UK PII: S0953-8984(98)85970-5

Positron lifetime spectroscopy and decomposition processes in commercial Al–Zn–Mg-based alloys

R Ferragut†, A Somoza† and A Dupasquier‡

† IFIMAT, Universidad Nacional del Centro de la Provincia de Buenos Aires, Pinto 399, 7000 Tandil, Argentina and Comisión de Investigaciones Científicas de la Provincia de Buenos Aires, Argentina

‡ Istituto Nazionale di Fisica della Materia, Dipartimento di Fisica, Politecnico di Milano, Piazza L da Vinci, 32, I-20133 Milano, Italy

Received 14 July 1997, in final form 27 November 1997

Abstract. Positron lifetime spectroscopy and Vickers microhardness measurements were used for studying the decomposition sequence of Al–Zn–Mg systems. Various microstructural changes (formation, dissolution and recuperation of GPII zones, formation of η'-particles) were induced by using isochronal annealing and multiple-step ageing thermal treatments. The experimental results give the following information: (a) changing the quenching temperature used for the initial homogenization treatment over the interval from -15 to $+55$ °C has no apparent effect on the subsequent behaviour of the alloy; (b) the hardening effect of natural ageing is positively correlated with the density of small and uniformly distributed GPII zones existing in the alloy at the end of the treatment; (c) the interruption in the reversion stage of artificial ageing at 150 °C is followed, at room temperature and at 70 °C, by a recovery that takes place with the same characteristic time constant t_C as governs GPII formation after the homogenization treatment; (d) the dependence of t_C on the temperature agrees with activation energies for the migration of the solute that depend on the concentrations of Mg and of the quaternary additions (Cu, Mn).

1. Introduction

Among age-hardenable aluminium alloys, the aluminium–zinc–magnesium system has been the object of particularly extensive investigations on account of its importance as a basis for the high-strength alloys of the 70XX series. The desirable mechanical properties of this class of alloys are due to structural inhomogeneities on a nanometric scale, which are formed at an intermediate stage in the evolution of the supersaturated solid solution (αSSS) toward an equilibrium structure, where the excess solute is segregated in the form of incoherent precipitates. The mechanism of nucleation of precipitates from supersaturated solid solutions governs the scale of the precipitate dispersion, which is the most important factor in determining the mechanical properties of the heat-treated alloy. Supersaturated Al–Zn–Mg alloys, left at room temperature, after a few days show an initial stage of decomposition (natural ageing), consisting in the formation of Guinier–Preston (GP) zones (solute-enriched structures coherent with the matrix). Thermal treatments at temperatures higher than room temperature (artificial ageing) may lead to complete decomposition, which normally occurs through the following sequence of stages: αSSS $\rightarrow$ spherical GP zones $\rightarrow$ ordered GP zones $\rightarrow$ transition phase η' (semi-coherent precipitates mainly with composition $MgZn_2$) $\rightarrow$ stable precipitates. However, the decomposition stages are developed and overlapping to a greater or lesser extent according to the details of the

0953-8984/98/173903+16$19.50

thermal treatments. Also the composition of the alloy is an important factor. In particular, the zinc:magnesium ratio has a pronounced effect on the mechanical properties, which is ascribable to its influence on the precipitation kinetics. The effect of minority elements and trace additions is also observable, but the mechanism of the action is still under discussion.

The reader may find information on earlier work relating to the Al–Zn–Mg system in the review by Löffler *et al* [1]. More recent studies, leading to the direct determination of the composition and microstructure of the GP zones and precipitates by atom-probe field-ion microscopy (APFIM) and high-resolution transmission electron microscopy (HRTEM), are described in references [2–4]. Good examples of state-of-the-art HRTEM studies of GP zones in other Al-based systems are to be found in [5, 6]. The continuing progress with advanced imaging techniques, however, does not put an end to interest in other well-established experimental methods: small-angle x-ray scattering (SAXS), small-angle neutron scattering (SANS), differential scanning calorimetry (DSC) and mechanical properties measurements; examples relating to Al–Zn and Al–Zn–Mg alloys can be found in references [7–9]. Positron annihilation spectroscopy (PAS) is also frequently used in the study of decomposition phenomena exhibited by age-hardenable alloys; more specifically, references [10–16] present PAS experiments on prepared Al–Zn and Al–Zn–Mg model alloys as well as on commercial Al–Zn–Mg systems.

In the present investigation we have combined positron lifetime spectroscopy with Vickers microhardness measurements in order to elucidate various aspects of the decomposition sequence of Al–Zn–Mg systems. We have obtained information on: (a) the effect of different quenching procedures on the further behaviour of the alloy; (b) the microstructural changes (formation, dissolution, reconstruction and growth of GP zones and of η'-precipitates) occurring as a consequence of pre-ageing and of a further ageing treatment; (c) the activation energies of the above processes; (d) the effect of the main secondary alloying element (the quaternary additive).

2. Experimental procedures

For the present study, we have chosen two alloys of the 70XX series, namely 7005 and 7012, which have about the same Zn:Mg ratio, but different quaternary additives (Mn in alloy 7005 and Cu in alloy 7012). The 7012 alloy has been the object of a recent study adopting the same techniques as are used in this investigation [16]. Some of the results presented in reference [16] will be given below for comparison with the new data. In detail, the compositions of the two systems are:

(i) alloy 7005: Al–4.6 wt% Zn–1.4 wt% Mg–0.5 wt% Mn (equivalent to Al–1.95 at.% Zn–1.60 at.% Mg–0.25 at.% Mn), also containing (in wt%) 0.1 Cr, 0.1 Zr, 0.03 Ti, Fe $<$ 0.4, Si $<$ 0.35 and Cu $<$ 0.1 (more details are given in [17]);

(ii) alloy 7012: Al–6.0 wt% Zn–2.0 wt% Mg–1.0 wt% Cu (equivalent to Al–2.58 at.% Zn–2.31 at.% Mg–0.44 at.% Cu), also containing (in wt%) 0.12 Zr, 0.10 Mn, 0.06 Ti, Fe $<$ 0.25, Si $<$ 0.15 and Cr $<$ 0.04; information on other properties of alloy 7012 is given in [18].

Specimens in the form of discs of 1.5 mm thickness were cut from a rod of 10 mm diameter using a low-speed diamond saw. The discs were thermally treated in various ways, as described in detail below. Heating at temperatures below 270 °C was carried out in a glycerine bath, as this ensures rapid temperature transients (about 3 s in the worst situation); due to the evaporation of glycerine, the thermal treatments at temperatures above 270 °C were performed in a resistive furnace. Cooling was performed by immersion in alcohol.

Cooling and heating rates were measured from temperature-versus-time plots taken on a Western Graphtec XY Recorder WX2300. At the end of each thermal treatment, the samples were given a metallographic polishing with diamond paste up to 1 μm followed by a dilute Keller etching. Lifetime spectra and hardness data were always taken at room temperature (20 °C).

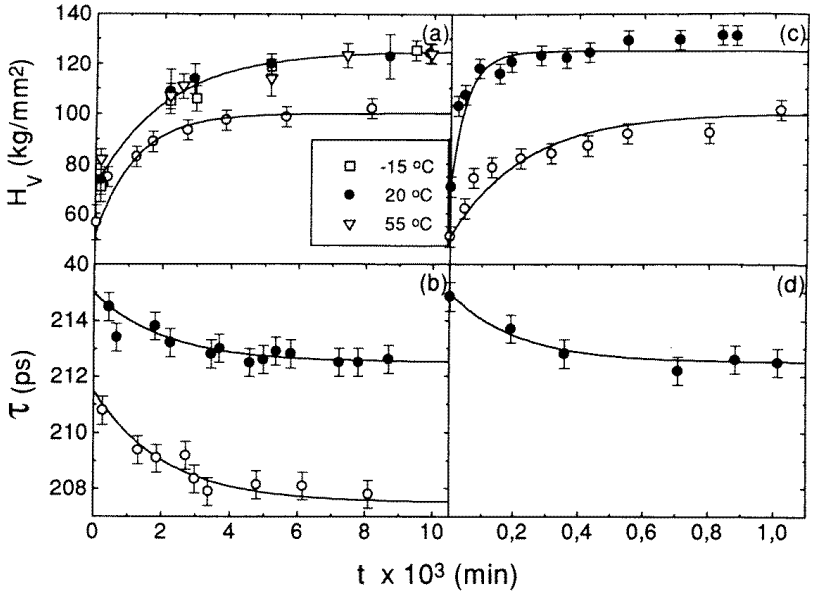

Figure 1. The evolution of the positron lifetime (τ) and the Vickers microhardness (H_V) at RT ((a) and (b)) and at 70 °C ((c) and (d)) after solution treatment for 7005 (lower curves) and 7012 (upper curves) alloys. The changes in the Vickers microhardness (for the 7012 alloy) for the different quenching temperatures −15 °C, 20 °C and 55 °C are also shown. The full lines represent fits to the experimental data with exponential curves (see the text).

The lifetime spectrometer was a fast–fast timing coincidence system with a time resolution (FWHM) of 255 ps. A 20 μCi source of ^{22}NaCl deposited on a thin Kapton foil (1.1 mg cm^{-2}) was sandwiched between two identical alloy specimens. The source contribution and the response function were evaluated by using the code RESOLUTION [19]. The source contributes to the spectra with only one component ($\tau_S = 382$ ps, $I_S = 10.5\%$). The lifetime spectra were analysed using the POSITRONFIT program [19]. After subtracting the source component, the spectra were satisfactorily analysed in terms of a single-lifetime component; in some cases the separation of two components is also possible, but this requires the use of constraints derived from the application of a trapping model with specific hypotheses made as regards the annihilation characteristics. We report below only the data obtained from free one-component fits, with the caveat that the apparent single lifetime τ has the meaning of an average over an unresolved complex lifetime spectrum. The total number of counts in each spectrum was about 10^6, accumulated over a time interval of 14 400 s. Measurements of the Vickers microhardness (H_V) were performed after each positron lifetime measurement by using a load of 100 g; the diagonal of the square explored by the indentor was about 40 μm.

3. Results

3.1. Homogenization

The homogenization treatment consists in heating the samples at a temperature above the solvus line for a time interval long enough for a uniform solid solution to be obtained; the heating stage is then followed by a rapid quenching in a cold bath. Differences in the quenching procedure (final temperature, quenching rate) affect the concentration of free vacancies in a way that could become manifest in the further evolution of the material. In order to study the effect, we have adopted the following homogenization treatment: (a) solubilization for 2 h at 475 °C in an air-circulating furnace; (b) quenching in an alcohol bath at different temperatures (20 °C, 55 °C and −15 °C). Within a rather large experimental scatter, we did not observe any influence of the bath temperature on the mean quenching rate ($|\mathrm{d}T_q/\mathrm{d}t| = 1900 \pm 400$ °C s^{-1}). At the end of the quenching, the samples were allowed to return to RT.

Figure 1 presents several sets of data relating to natural ageing, which will be discussed in section 3.2. For the moment, just look at the upper curve in part (a) of this figure: here we show the results of Vickers microhardness measurements for alloy 7012, taken for samples quenched at different temperatures (some of the RT data are from reference [16]). No evidence of a possible effect of the quenching bath temperature emerges from these data.

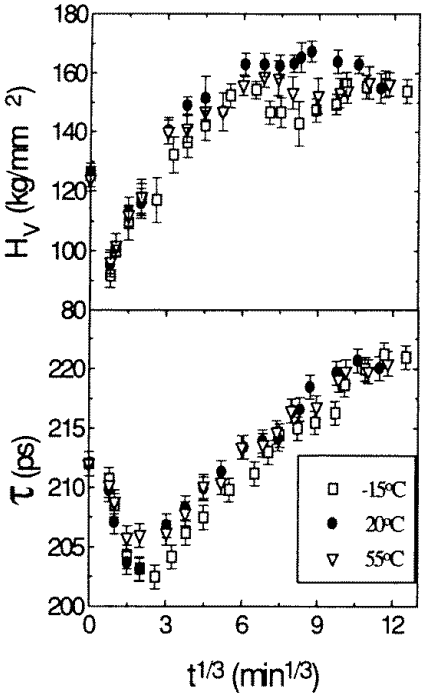

Figure 2. The evolution of the microhardness and positron lifetime of alloy 7012 during ageing at 150 °C after a solubilization treatment for 2 h at 475 °C followed by different quenching processes at 55 °C (open triangles), 20 °C (full circles) and −15 °C (open squares). After quenching and before ageing at 150 °C, the samples were naturally aged for five days at RT.

The very limited variation of the positron lifetime that occurs during natural ageing (see figure 1(b)) discouraged us from making any attempt to observe second-order variations related to a change of the quenching temperature. Instead, we searched for an effect of the quenching temperature on the evolution of H_V and τ during artificial ageing, given as the second step of a treatment performed at two different temperatures. Artificial ageing is discussed below (section 3.3), but we anticipate here (figure 2) some data for alloy 7012, relating to the effect of changing the temperature of the quenching bath. Figure 2 shows small and irregular differences, probably accidental, but without correlation with the quenching temperature.

We conclude that the possible differences in the microstructure of the material due to a change in the temperature of the quenching bath from -15 °C to $+55$ °C do not affect the results of the measurements of the present work. For this reason, all of the data presented below refer only to RT quenching.

3.2. Pre-ageing

Two-step ageing treatments constitute a standard procedure used for improving the mechanical characteristics of age-hardenable alloys after the initial homogenization treatment. The first step (pre-ageing) is an isothermal treatment at RT or at another temperature sufficiently low that the nucleation of incoherent particles is avoided. During this stage, a uniform and fine dispersion of GP zones is formed. We have studied pre-ageing at RT and at 70 °C. Data relating to the time evolution of the Vickers microhardness H_V and of the positron lifetime τ are presented in figure 1 (including data for alloy 7012 from reference [16]). Figures 1(a) and 1(c) show a strong increase of H_V, which reaches an apparent saturation at about 100% above the initial value. Figures 1(b) and 1(d) show a small decrease of τ, which reaches an apparent saturation 2 or 3 ps below the initial value. The RT dependences of τ on the ageing time are almost identical for the two alloys; the comparison is impossible at 70 °C since the scatter of the experimental data for alloy 7005 (not shown in the figure) was of the same magnitude as the expected variation of τ (a few picoseconds). We have fitted the experimental data presented in figure 1 with curves corresponding to exponential time laws of the form

$$F = F_f - (F_f - F_i)\mathrm{e}^{-t/t_C} \tag{1}$$

where F represents either H_V or τ, the subscripts f and i represent the final and initial values of these parameters, and t_C is a characteristic time. The best-fit values for t_C depend on the alloy studied and on the temperature, but we could fit the microhardness data and positron lifetimes with the same t_C. The results of the combined t_C-fit for the two series of data are given in table 1.

3.3. Artificial ageing

Artificial ageing is the second step of the classical two-step ageing treatments used on age-hardenable alloys. It is a treatment performed at a temperature sufficiently high to produce a rapid coarsening of the GP zones formed during pre-ageing. After reaching a critical size, the GP zones are eventually transformed into semi-coherent precipitates (η'-particles). Maximum hardness is obtained with a fine distribution of small η'-particles; overly long treatments lead to over-ageing, corresponding to an advanced stage of decomposition of the alloy, with the formation of a coarse distribution of incoherent equilibrium precipitates (η-particles).

Table 1. Characteristic times obtained by fitting the data of figure 1 with exponential functions of the form given by equation (1) for the process of the microstructural evolution at RT and 70 °C after solution heat treatment and quenching. The relative errors are below 15%.

Pre-ageing		
	t_C (min)	
Alloy →	7012	7005
Temperature ↓		
20 °C	2100	1150
70 °C	52	230

We have studied the evolution of the two alloys during artificial ageing implemented after a pre-ageing of five days at RT (from the results presented in section 3.2, we see that five days is enough time for a stage of apparent saturation of the increase of τ and H_V to be reached). In order to obtain guidance as regards the choice of the temperature of the ageing treatment, we have preliminarily observed the variations of τ and H_V that occur during an isochronal accumulative annealing treatment for 30 min at temperatures increasing from 40 °C/50 °C to 300 °C/340 °C, depending on the alloy. At the end of each heating period, the samples were quenched in alcohol at RT. The measurements of H_V and τ were performed immediately after quenching (it will be shown below that this is an important detail).

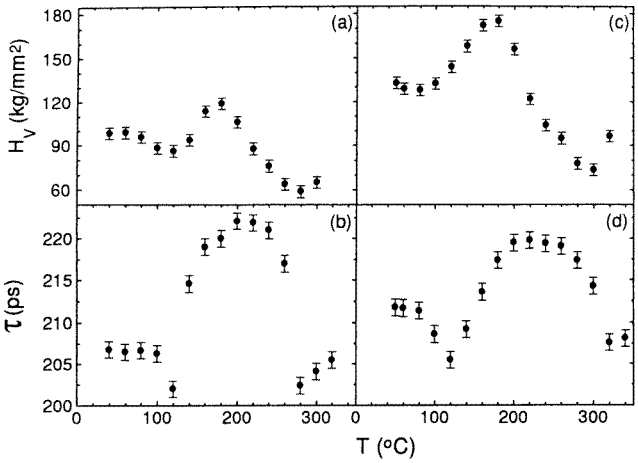

Figure 3. The evolution of the microhardness H_V and positron lifetime τ during an isochronal heat treatment: alloy 7005, (a) and (b); alloy 7012, (c) and (d).

Figure 3 shows the evolution of H_V and τ for alloys 7005 (panels (a) and (b)) and 7012 (panels (c) and (d)) during the isochronal annealing. Both parameters display an initial decrease and reach a minimum for temperatures between 90 °C and 110 °C, then increase up to the maximum values of $\tau = 222$ ps and $H_V \approx 120$ kg mm^{-2} for alloy 7005 and $\tau = 220$ ps and $H_V \approx 175$ kg mm^{-2} for alloy 7012. The positions of the maxima of the curves are almost the same for the two alloys: about 175 °C for H_V and about 215 °C for τ. At higher annealing temperatures (≈275 °C for the 7005 alloy and ≈310 °C for the 7012 alloy) τ and H_V fall back to near their initial values.

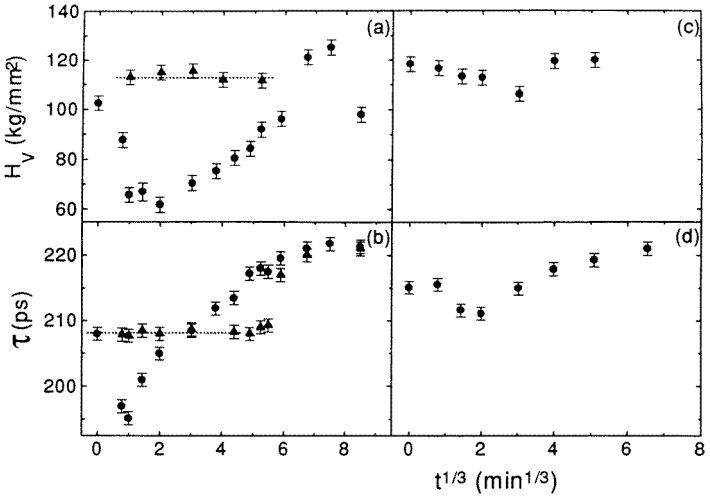

Figure 4. Changes in the microhardness H_V and positron lifetime τ of alloy 7005 during ageing at 150 °C after five days' pre-ageing at RT ((a) and (b)) and at 70 °C ((c) and (d)). The full circles represent the results of prompt measurements and the triangles represent the results of delayed measurements (see the text). The dotted line is a visual guide.

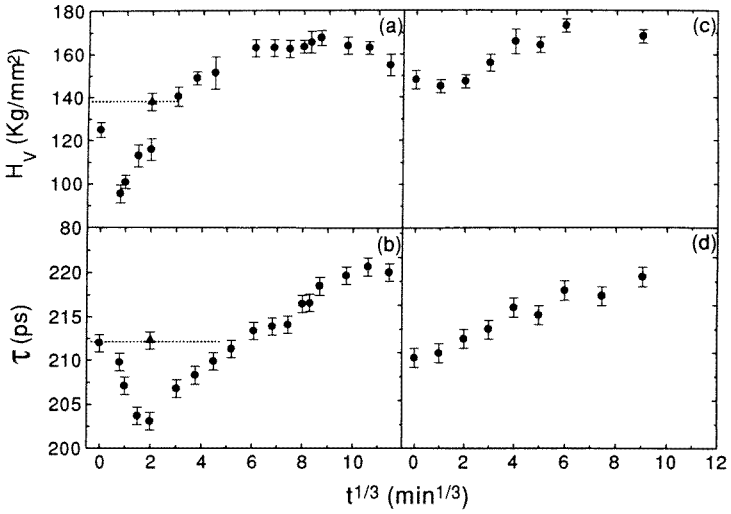

Figure 5. Changes in the microhardness H_V and positron lifetime τ of alloy 7012 during ageing at 150 °C after five days' pre-ageing at RT ((a) and (b)) and at 70 °C ((c) and (d)). The full circles represent the results of prompt measurements and the triangles represent the results of delayed measurements (see the text). The dotted line is a visual guide.

On the basis of the above results, the isothermal ageing was performed at 150 °C, i.e. at a temperature in the middle of the range in which the rapid increase of τ and H_V shown in figure 3 indicates the onset of precipitation. The treatment was interrupted after a variable time t and the samples were alcohol quenched at RT. The positron lifetime τ and the microhardness H_V measured at RT are plotted as functions of the ageing time in

figures 4 and 5 for alloys 7005 and 7012, respectively. The timescale chosen in these figures is $t^{1/3}$; this is a convenient choice for representing a structural evolution occurring in a coalescence regime, as implied by the Lifshitz–Slyozov–Wagner coarsening theory (see [14] for a discussion of the validity of this theory as a description of the coarsening of GP zones).

Panels (a) and (b) on the left-hand side of figures 4 and 5 are for samples pre-aged at RT for five days (the results for alloy 7012 are from reference [16]), whereas panels (c) and (d) on the right-hand side are for samples pre-aged for five days at 70 °C. The figures contain data points represented either by full circles or by triangles: full circles correspond to measurements initiated immediately after the ageing treatment and concluded in a few hours (*prompt measurements*), while triangles represent data taken at least five days after the interruption of the thermal treatment (*delayed measurements*). It is evident from these data that the properties of the alloy, modified by artificial ageing, may revert in a few days to their initial values if the thermal treatment is interrupted in the initial stage. More information on this recovery process will be given below (section 3.4). For the moment, we ask readers to concentrate their attention on the results of the prompt measurements. Our new data confirm the results of reference [16], indicating that the initial effect of the artificial ageing is a decrease of the hardness and of the positron lifetime. The decrease is followed by an increasing stage that eventually brings both parameters to a new maximum above the initial value. The temperature of the pre-ageing treatment is important: a comparison of panels (a) and (b) on the left-hand side of figures 4 and 5 (pre-ageing at RT) with panels (c) and (d) on the right-hand side of the same figures (pre-ageing at 70 °C) shows that the variations occurring in the second ageing step after the pre-ageing at 70 °C are smaller than the corresponding variations observed for samples pre-aged at RT. The treatment at 70 °C probably anticipates part of the transformation process occurring during the second ageing step at 150 °C: at the end of the 70 °C treatment, H_V and τ are already above the value obtained with a RT pre-ageing, and, when the temperature is increased to 150 °C, the increasing stage is reached on passing through a very shallow minimum (which is not even always present). In contrast, the temperature of the pre-ageing does not significantly affect the maximum values reached by H_V and τ.

3.4. Recovery after partial ageing

As noted above, the differences between the results of prompt and delayed measurements, shown in figures 4 and 5, indicate that the modifications of the properties of the alloy due to artificial ageing are only temporary if the thermal treatment is interrupted at an early stage. The existence of a recovery phenomenon was already established in our previous work on alloy 7012 [16]; the new data for alloy 7005 suggest that this phenomenon is a common characteristic for the 70XX series. We recall that the same behaviour is also known for other Al-based alloys [20]. Recovery is faster in alloy 7005 than in alloy 7012; this difference has provided us with the possibility of collecting many data in a reasonable time. We thus have in figures 4(a) and 4(b) enough points (triangles) to enable us to draw the lines that display the permanent effects of artificial ageing. These lines may have practical applications: for instance, the rather sharp edge at $t^{1/3} \approx 6.8$ min$^{1/3}$ of the curve drawn through the triangles in figure 4(b) gives a potentially useful indication of the minimum value of the time ($t \approx 314$ min) needed to obtain the stabilization of the ageing effect. New information also coming from figure 4(b) is that the lines connecting the circles or the triangles (i.e. the results of prompt or delayed measurements, respectively) cross at a certain point ($t^{1/3} \approx 3.2$ min$^{1/3}$); this means that the recovery of

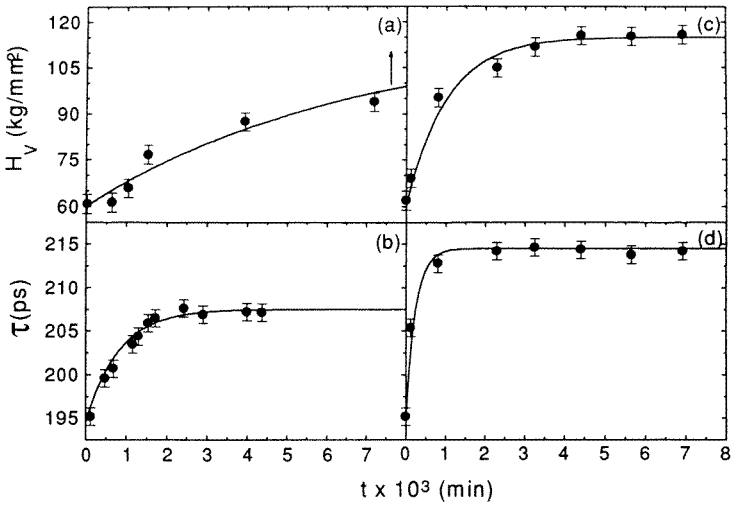

Figure 6. The evolution of the microhardness and positron lifetime for alloy 7005 occurring during a final ageing treatment at RT ((a) and (b)) and at 70 °C ((c) and (d)) after the interruption of the ageing at 150 °C after 1 min (the minimum of τ in figure 4). The arrow indicates that the fitting with the exponential function of equation (1) is made under the assumption that the asymptotic value of H_V at RT is the same as was observed at 70 °C.

the positron lifetime can begin not only from below but also from above the asymptotic value.

In order to investigate the microscopic mechanisms that govern the recovery, an important piece of information is how a change in the temperature may affect the recovery rate. The data relating to alloy 7012 are given in reference [16]. We give the corresponding data relating to alloy 7005 in figure 6, showing the evolution of τ and of H_V at RT and at 70 °C for samples pre-aged at RT for five days, then aged at 150 °C for the time needed to bring τ to its minimum (1 min).

The curves through the experimental points are a fit with an exponential function of the form given by equation (1), which defines a characteristic time. Best-fit values of the characteristic times t'_C, obtained from H_V-data, and t''_C, obtained from τ-data, are given in table 2, which also includes the results from reference [16] for alloy 7012.

Table 2. Characteristic times obtained by fitting the hardness (H_V) and positron lifetime (τ) experimental data with exponential functions of the type of equation (1) for the process of the microstructural recuperation at RT and 70 °C after the interruption of artificial ageing at an early stage. The relative errors are below 15%.

Recovery after artificial ageing				
	t'_C (min) (from H_V-measurements)		t''_C (min) (from τ-measurements)	
Alloy → Temperature ↓	7012	7005	7012	7005
20 °C	42 000	6490	30 000	810
70 °C	1020	1020	960	240

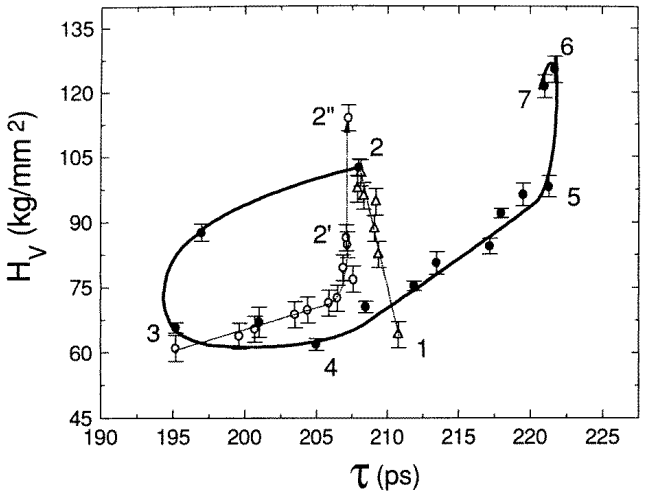

Figure 7. The evolution of alloy 7005 represented in the H_V–τ plane. Point 1 represents the condition after solubilization and quenching in cold water. The dotted line from 1 to 2 represents pre-ageing at RT (for clarity, we have omitted here some of the data reported in figure 3 to avoid there being too many overlapping points in the H_V–τ plane). The full line from 2 to 7 represents ageing at 150 °C. Point 3 represents the condition reached after 1 min at 150 °C. The dashed line from 3 to 2′ represents the evolution that occurs if the treatment at 150 °C is interrupted at point 3 and the sample, rapidly brought to RT, is left to age at this temperature. Horizontal error bars are not shown in this plot, but the equivalent information is given by means of vertical error bars for τ in figures 1, 4 and 6.

4. Discussion

Before proceeding to a discussion of the results presented in section 3, it is convenient to recall very briefly the mechanism that makes positron lifetimes sensitive to the microstructure of the alloy. It is well known that a positron thermalized in a metal may be trapped by defects that produce an empty space in the lattice (vacancies, vacancy clusters, voids, misfit regions). Since the lifetime of a positron trapped in an open space is longer that the lifetime of a free positron in the bulk of the material, trapping may manifest itself through the increase of the average positron lifetime; for instance, trapping at vacancies in aluminium gives a lifetime of 245 ps [21] whereas the bulk lifetime is ≈164 ps [22]. Trapping may also occur in a cluster of solute atoms containing no open spaces, provided that the positron affinity of the solute is bigger than the positron affinity of the matrix and the radius of the cluster is above a critical limit; in this case, however, the lifetime of a trapped positron may be even shorter than the lifetime of a free positron. It has been convincingly shown by Dlubek and co-workers [10–13] that in Al–Zn–Mg alloys the positrons can be trapped by GP I zones (clusters of pure or nearly pure Zn, containing no vacancies), by GP II zones (clusters of Zn and Mg atoms, associated with structural vacancies) and by misfit regions at the incoherent boundaries of the precipitates. In the second and in the third case, trapping produces an increase of the lifetime. The sensitivity of the positron lifetime to GP zones and to precipitates gives, in some situations, an apparent correlation of τ with the microhardness H_V, which is also increased in the presence of GP zones and precipitates that hinder the motion of the dislocations. However, the two variables have no direct physical connection, and their correlation is only coincidental: in fact they do not respond with the

same sensitivity to the changes in the distribution and in the concentration of GP zones and of precipitates; moreover, τ can be affected by defects that have no influence on H_V and vice versa. In our earlier consideration of the absence of a true correlation, we gave, in reference [16], a representation of the structural evolution of alloy 7012, using τ and H_V as independent coordinates. Figure 7 shows the same kind of diagram for alloy 7005. We use this diagram as a guide for the interpretation of the data and for making a comparison between the two alloys.

4.1. Pre-ageing

Figure 1 shows that during pre-ageing at RT and at 70 °C, τ decreases and H_V increases. In figure 7, this transformation appears as a straight line with negative slope. This behaviour, which contrasts with the apparent positive correlation shown in figures 3–5, had already been observed (but only at RT) and discussed in our previous work on alloy 7012 [16]. Our interpretation is that the effect arises from the formation of GP II zones at the expense of the vacancy clusters and of the vacancy–solute pairs that survive in the alloy at the end of the homogenization treatment. The modest decrease of the positron lifetime would thus be the result of a slight imbalance of two opposite contributions: reduction of the trapping at vacancy clusters and at isolated vacancy–solute pairs, partially compensated by the increase of trapping in GP II zones. Microhardness, in contrast, is insensitive to point-like defects; thus, its increase arises only from the formation of GP zones. We must note that, in contrast with what was expected from our interpretation, Zn- and Mg-rich GP zones were not detected [3] after natural ageing by APFIM in alloy 7018, which has a composition very similar to that of alloy 7012. However, we find decisive support of our interpretation in a preliminary HRTEM study of alloy 7012, which leaves no doubt as regards the presence of GP zones and gives no evidence of homogeneous formation of precipitates after extensive ageing at room temperature [23]. SAXS data on the ternary alloy Al–6.1 wt% Zn–2.35 wt% Mg show the presence of GP zones with a Guinier radius of 0.6 nm after three days of natural ageing [9].

The data taken at two different temperatures (see figure 1 and table 1) can be used for obtaining information on the microscopic mechanism governing the structural transformations that occur during pre-ageing. The coincidence of the time constants t_C that characterize the time dependence of H_V and τ shows that the microstructural changes affecting the two variables are produced by the migration of the same atomic species or solute–vacancy complex. Transport of solute atoms or complexes in a solid solution is a thermally activated process; the characteristic time should thus depend on the temperature T and on the activation energy E as expressed by the law [24]

$$t_C = t_0 \exp(E/kT) \tag{2}$$

where t_0 is a constant and k is the Boltzmann constant. Using equation (2) and the best-fit data for t_C, we obtain $E = 0.66 \pm 0.05$ eV for alloy 7012 (from microhardness and positron lifetime data) and $E = 0.29 \pm 0.04$ eV for alloy 7005 (from microhardness data only, since we do not have reliable positron lifetime data taken at 70 °C for this alloy). The different values of the activation energy indicate that the diffusing species are not the same for the two alloys. We shall return to this point below.

4.2. Artificial ageing

It is known that the alloys of the series 70XX that contain Cu as a quaternary component (e.g. alloys 7012, 7018 and 7075) have better mechanical properties than those containing

Mn instead of Cu (e.g. alloy 7005) [25]. Our data not only confirm this result (figure 3 shows that upon peak-ageing, H_V is about 50% higher for alloy 7012 than for alloy 7005), but also suggest that this difference may be related to the distribution of GP II zones at the end of the pre-ageing phase (figure 1 shows that the positron lifetime is higher for alloy 7012 ($\approx$212 ps) than for alloy 7005 ($\approx$208 ps), indicating a GP II distribution that is denser and more finely distributed in the first case than in the second). This indication is consistent with the decisive effect of copper in nucleating and stabilizing the early stages of GP II zone formation in Al–Zn–Mg–Cu alloys (see [4] and references therein). The addition of Mn as a quaternary element to an Al–Mg–Zn alloy also contributes to the hardening, but the microstructural mechanism is not related to the GP II distribution: Mn forms dispersoids which restrict dislocation motion and consequently increase the strength of Al–Zn–Mg alloy [26]. However, Mn dispersoids do not affect the positron lifetime, because positron trapping is energetically forbidden (the positron affinity for Mn is lower that the affinity for the Al matrix of the alloy [27]).

Apart the above quantitative difference, figures 4 and 5 show that the evolutions of the two alloys during artificial ageing are qualitatively the same. We may follow in figure 3 the evolution of the two alloys during the isochronal treatment. From considering the variations of H_V, we observe a sequence of three phases: (a) softening (the *reversion trough*), down to a minimum microhardness 5–10% below the initial value at the end of the pre-ageing; (b) hardening, up to a maximum microhardness 20–30% (*peak ageing*) above the initial value; (c) softening (*over-ageing*), down to a final value of microhardness 40–50% below the initial value. The positron lifetimes also evolve in a sequence of three phases: (a′) decreasing lifetime (to a minimum 3–4% below the initial value); (b′) increasing lifetime (to a maximum 4–8% above the initial value); (c′) decreasing lifetime, going down to $\sim$5% below the initial value. In figure 7, the evolution of alloy 7005 during isothermal ageing at 150 °C is represented by the curved line from point 2 to point 7 (through points 3–4–5–6). Looking at the evolution of H_V, we find again: (a) softening (from point 2 to point 4); (b) hardening (from 4 to 6); (c) softening (from 6 to 7). For the positron lifetime, we find: (a′) a decreasing lifetime (from 2 to 3); (b′) an increasing lifetime (from 3 to 6); (c′) a decreasing lifetime (from 6 to 7). The sequences (a)–(b)–(c) and (a′)–(b′)–(c′) always retain the same ordering, but are not exactly coincident; this means that H_V and τ reflect the same microstructural transformations, but with different sensitivities. We identify these transformations as follows: (i) partial reversion, i.e. dissolution of the smallest GP II zones; (ii) coalescence, i.e. growth of the biggest GP II zones at the expense of the smallest ones, eventually leading to transformation of the GP II zones into η'-particles; (iii) dissolution of the η'-phase, leading to the formation of a coarse distribution of η-particles. The three transformations occur in sequence, but with considerable overlap between (i) and (ii); indeed, HRTEM images, taken for alloy 7012 in conditions corresponding to the bottom of the reversion trough, already show incipient formation of the η'-phase [23]. SAXS and TEM results for the alloy Al–6.1 wt% Zn–2.35 wt% Mg show the presence of particles with a radius growing from about 1.5 nm after 30 min at 160 °C to about 2.6 nm after 200 min [9]. Transformation (i), which reduces the hardness as well as the positron trapping, is the dominant factor during phases (a) and (a′); transformation (ii) becomes dominant during phases (b) and (b′); finally, transformation (iii) coincides with phases (c) and (c′). The same interpretation has been proposed in reference [16] for alloy 7012. However, the weights of the microstructure transformations affecting H_V and τ cannot be the same in the two alloys, since the sequences of the phases are displaced in such a way that the H_V/τ diagrams curl in opposite directions. The different sequences of the phases are most probably related to the size distribution of the GP zones and to the early precipitation of the η'-phase, which

is affected by the composition of the alloy. Similar compositional effects were observed in the reversion stage of Al–Cu–Li–Ag–Mg systems [20, 28].

Our interpretation does not call into question the formation of GP I zones as a possible reason for the decrease of the positron lifetime observed in phase (a′). This point deserves comment. Since positron trapping in GP I zones was observed by Dlubek *et al* in prepared Al–Zn–Mg, the possibility of the formation of GP I zones cannot be excluded *a priori*, although alloys 7005 and 7012 contain less Zn than the alloys studied in reference [10]. Considering the short lifetime connected with the GP I zones (155 ps [10]), one might wonder whether the decrease of the average lifetime observed in phase (a′) could actually be related to the increase of trapping in GP I zones in competition with GP II zones. However, this explanation must be discarded for two reasons: (1) formation of more GP zones would not explain the softening observed in phase (a), which partially overlaps with phase (a′); (2) the isothermal ageing was performed at a temperature (150 °C) that is too high for the formation of GP zones (taking into account the compositions of our alloys, TEM results [1] indicate that the upper limits above which no GP zone formation can be detected are $T_H \approx 105$ °C for alloy 7005 and $T_H \approx 125$ °C for alloy 7012; complete dissolution of the GP zones occurs at 145 °C and at 170 °C for alloys 7005 and 7012, respectively).

Phases (c) and (c′), related to the transformation $\eta' \rightarrow \eta$, are much more evident during the isochronal treatment than during the isothermal treatment at 150 °C. At this temperature, the transformation $\eta' \rightarrow \eta$ is only marginal; we see from figure 3 that the fall of H_V and τ begins at ≈180–190 °C and reaches a minimum or a plateau at ≈290–300 °C. This final temperature coincides with the temperature of transformation $\eta' \rightarrow \eta$ indicated in the Al–Zn–Mg phase diagram for alloys with the same zinc and magnesium contents as the 7005 and 7012 alloys [29].

4.3. Recovery after reversion

The explanation that we give here for the recovery of the initial values of H_V and τ, observed for samples partially aged at 150 °C, quenched and left to re-age at RT (or at 70 °C) is the same as that discussed in reference [16]. We attribute the phenomenon to a recuperation (renewed formation) of GP II zones. The solute that forms these zones comes from the dissolution of the small GP zones taking place during the reversion stage. The recuperation of the GP zones is necessarily incomplete, because only a fraction of the solute initially contained in the dissolved zones is available; the remaining part is absorbed during reversion by more stable structures (large GP zones or η'-particles, in proportions depending on the composition of the alloy). These structures survive after quenching and combine their effects with those of the recuperated GP II zones, but combination in this case does not mean addition. In the case of the positron lifetime, for instance, we can explain the rather surprising 'recovery from above', displayed in figure 4(b) for the interval $3.2\ \text{min}^{1/3} \leqslant t^{1/3} \leqslant 6.8\ \text{min}^{1/3}$, as the effect of competition between weak trapping in a small concentration of η'-particles and strong trapping in a dominant concentration of recuperated GP II zones.

With the help of equation (2), the data relating to the characteristic times reported in table 2 give us access to the activation energies relative to the transport of the solute. The results are: (a) for alloy 7005, $E = 0.32 \pm 0.05$ eV from hardness measurements and $E = 0.21 \pm 0.05$ eV from positron lifetime measurements; (b) for alloy 7012, $E = 0.64 \pm 0.05$ eV from hardness measurements and $E = 0.59 \pm 0.05$ eV from positron lifetime measurements [16]. The difference between the values obtained by the two

techniques is below the error limits for alloy 7012 and barely above the error limits for alloy 7005. This fact might be significant, since the transformations occurring in alloy 7005 with the heat treatment at 70 °C are probably not exactly the same as those that occur at RT. Indeed, the difference between the saturation values of the positron lifetime at RT and at 70 °C (compare figures 6(b) and 6(d)) seems to indicate that at 70 °C, together with the recuperation of GP zones, there is an incipient formation of η'-particles.

Table 3. Activation energies for solute diffusion, obtained from the evolution of the Vickers microhardness and positron lifetime at RT and at 70 °C. The error limits are of the order of 0.05 eV.

Activation energies		
	E (eV)	
Alloy → Process ↓	7005	7012
Evolution after solubilization (pre-ageing)	0.29	0.66
Recovery after reversion (recuperation)	0.27	0.62

4.4. On the meaning of the different values of the activation energies

We have collected in table 3 the various values of the activation energies mentioned in sections 4.1 and 4.3. We have ignored here the possible systematic effects mentioned above for explaining the small differences between PAS and microhardness results, and we have taken the mean of the two values.

The comparison of the values reported in the table shows that: (a) within the error limits, the same activation energy governs the evolution of each alloy after the homogenization treatment as well as after the interruption of the artificial ageing at 150 °C; (b) the activation energies are not the same for the two alloys. From point (a) we conclude that the transformation is the same in the two cases, in spite of the different thermal histories of the samples. This is consistent with our interpretation, which in both cases calls into question the formation of GP II zones. The conclusion that must be drawn from point (b) is that the diffusing species that limit the nucleation and the formation of the GP II zones are not the same in the two alloys. Identification of these species may be attempted on the basis of a comparison with the following data reported in the literature for prepared Al–Zn and Al–Zn–Mg alloys:

(a) migration of the Zn–vacancy complex (ZnV): 0.42 eV in Al–Zn [30] and in Al–Zn–Mg [31] with an atomic concentration ratio C_{Mg}/C_{Zn} below 0.38;

(b) migration of the Zn_2–vacancy complex (Zn_2V): 0.21 eV for Al–Zn–Mg [31] with an atomic concentration ratio C_{Mg}/C_{Zn} between 0.38 and 1.7 (the atomic concentration ratio is 0.82 for alloy 7005 and 0.90 for alloy 7012);

(c) migration of the Mg–vacancy complex (MgV): 0.60 eV (see [1] and references therein).

These data suggest Zn_2V as the dominant diffusing species for alloy 7005 and MgV for alloy 7012. The reason for the dominance of one diffusing species in one alloy and another species in the other alloy must lie in the respective chemical compositions. Possible

microscopic mechanisms that explain the effect of the composition on the migration of the solutes were discussed in [31]. Alloys 7005 and 7012 have almost the same magnesium-to-zinc ratios; the main points of difference lie in: (a) the absolute value of the Mg content (1.4 wt% in alloy 7005, 2 wt% in alloy 7012), a factor that seems to influence the diffusion processes rather strongly in special cases [30, 32]; (b) the quaternary element (Mn in alloy 7005, Cu in alloy 7012). It is known that additions of Cu to Al–Zn–Mg alloys favour the formation of GP II zones and delay the rate of η'-precipitation, while Mn acts in the opposite way [33]. The microscopic action of Cu could be the capture of a number of vacancies, thereby reducing the quantity available for the formation of movable complexes with the main solute elements. On raising the Mg content, the residual vacancies should be mostly captured by Mg atoms, thus reducing the concentration of the Zn_2V complex.

5. Conclusions

In the present paper we have discussed the evolution of age-hardening alloys of the series 70XX, from the homogenized condition to the first symptoms of over-ageing; we have analysed separately the various stages of the thermal treatment which is normally adopted for improving the mechanical properties of this class of alloys. We have adopted two techniques, namely the measurement of the Vickers microhardness and that of the positron lifetime, which give complementary information on the microscopic phenomena that occur during the thermal treatments and on their macroscopic effect on the mechanical properties.

This study confirms the results of a more limited investigation previously performed on alloy 7012 [16], extends the analysis to different thermal treatments and compares results for alloys of different compositions. According to our interpretation, the main results of the present work give the following information:

(a) *homogenization:* a limited modification of the quenching temperature, without important changes of the quenching rate, does not affect the further evolution of the material;

(b) *pre-ageing at RT (or 70 °C):* the combined effect of the annealing of point-like defects with the formation of GP II zones results in an apparent negative correlation between the microhardness and the positron lifetime; the comparison of two different alloys indicates that, at the end of the treatment, the alloy with the greatest microhardness contains a denser and more finely distributed population of GP II zones;

(c) *artificial ageing*: the existence of a 'reversion trough' in the initial stages of the treatment, related to the dissolution of small GP II zones and partially reversible at RT or at 70 °C, is not a property specific to alloy 7012, but is found also for other alloys of the 70XX series; in the later stages of the treatment, the hardening is determined by an irreversible transformation of GP II zones in η'-precipitates;

(d) *recovery after reversion*: the material left at the bottom of the reversion trough in a supersaturated state by the interruption of the artificial ageing evolves by means of the same mechanisms as govern the evolution after complete solubilization; some of the GP II zones dissolved at high temperature are formed again;

(e) *over-ageing*: the decrease of the microhardness, of modest extent with artificial ageing at 150 °C, becomes dramatic if temperatures above 200 °C are reached in an isochronal treatment of 30 min; the positron lifetimes indicate coarsening of the precipitates;

(f) *compositional effects*: different compositions lead to different transformation rates and different activation energies; the presence of Cu and of a high Mg concentration favour the formation of Mg–vacancy complexes rather than Zn_2–vacancy complexes.

Acknowledgments

This work was partially supported by the Consejo Nacional de Investigaciones Científicas y Técnicas (PIP No 318/97), Comisión de Investigaciones Científicas de la Provincia de Buenos Aires, Fundación Antorchas and Secretaria de Ciencia y Técnica de la UNCentro (Argentina)

References

[1] Löffler H, Kovacs Y and Lendvai J 1983 *J. Mater. Sci.* **18** 2215
[2] Ortner S R, Grovenor C R M and Shollock B A 1988 *Scr. Metall.* **22** 839
[3] Ortner S R and Grovenor C R M 1988 *Scr. Metall.* **22** 843
[4] Mukhopadhyay A K, Yang Q B and Singh S R 1994 *Acta Metall. Mater.* **42** 3083
[5] Ringer S P, Sakurai T and Polmear I J 1997 *Acta Mater.* **45** 3731
[6] Karlik M and Jouffrey B 1997 *Acta Mater.* **45** 3251
[7] Guilarducci de Salva A, Simon J P, Livet F and Guyot P 1987 *Scr. Metall.* **21** 1061
[8] Chinh N Q, Kovács Zs, Reich L, Székely F, Illy J and Lendvai J 1977 *Z. Metallk.* **88** 609
[9] Deschamps A, Bréchet Y, Guyot P and Livet F 1977 *Z. Metallk.* **88** 601
[10] Dlubek G, Krause R, Brümmer O and Plazaola F 1986 *J. Mater. Sci.* **21** 853
[11] Dlubek G 1984 *Cryst. Res. Technol.* **19** 1319
[12] Dlubek G, Brümmer O, Hautojärvi P and Yli-Kauppila J 1981 *J. Phys. F: Met. Phys.* **11** 2525
[13] Dlubek G and Gerber W 1991 *Phys. Status Solidi* b **163** 83
[14] Abis S, Biasini M, Dupasquier A, Sferlazzo P and Somoza A 1989 *J. Phys.: Condens. Matter* **1** 3679
[15] Dupasquier A, Folegati P, Rolando A, Somoza A and Abis S 1995 *Mater. Sci. Forum* **175–178** 351
[16] Ferragut R, Somoza A and Dupasquier A 1996 *J. Phys.: Condens. Matter* **8** 8945
[17] *Metals Handbook* 1979 9th edn, vol II (Metals Park, OH: American Society of Metals) pp 123–5
[18] Di Russo E and Buratti M 1979 *Metall. Italiana* **10** 449
[19] Kirkegaard P, Pedersen N J and Eldrup M 1989 *PATFIT-88 Program* Risø National Laboratory, M-2740
[20] Gayle F W, Heubaum F H and Pickens J R 1990 *Scr. Metall. Mater.* **24** 79
[21] Schaefer H-E, Gugelmeier R, Schmolz M and Seeger A 1987 *Mater. Sci. Forum* **15–18** 111
[22] Dupasquier A, Romero R and Somoza A 1993 *Phys. Rev.* B **48** 9235
[23] Somoza A 1997 *Mater. Sci. Forum* **255–257** 86
[24] Panseri C and Federighi T 1963 *Acta Metall.* **11** 575
[25] *Metals Handbook* 1979 9th edn, vol II (Metals Park, OH: American Society of Metals) pp 124, 130
[26] Jo B L, Park D S and Nam S W 1996 *Metall. Trans.* A **27** 490
[27] Puska M J, Lanki P and Nieminen R M 1989 *J. Phys.: Condens. Matter* **1** 6081
[28] Kumar K S, Brown S A and Pickens J R 1996 *Acta Mater.* **44** 1899
[29] Mondolfo L F 1976 *Aluminium Alloys: Structure and Properties* (London: Butterworth) pp 577–90
[30] Jürgens G, Kempe M and Löffler H 1974 *Phys. Status Solidi* a **21** K39
[31] Jürgens G, Kempe M and Löffler H 1974 *Phys. Status Solidi* a **25** K73
[32] Löffler H and Fabian H-G 1995 *Structure and Structure Development of Al–Zn Alloys* ed H Löffler (Berlin: Akademie) p 352
[33] Kelly A and Nicholson R B 1963 *Prog. Mater. Sci.* **10** 216